35th Annual International Conference of the IEEE EMBS
Osaka, Japan, 3 - 7 July, 2013

# Comparison of Simulated and Clinical Intracardiac Electrograms

Matthias W Keller[1], Steffen Schuler[1], Armin Luik[2], Gunnar Seemann[1], Christopher Schilling[1], Claus Schmitt[2], Olaf Dössel[1]

*Abstract*— **Intracardiac electrograms are the key in understanding, interpretation and treatment of cardiac arrhythmias. However, electrogram morphologies are strongly variable due to catheter position, orientation and contact. Simulations of intracardiac electrograms can improve comprehension and quantification of influencing parameters and therefore reduce misinterpretations. In this study simulated intracardiac electrograms are analyzed regarding tilt angles of the catheter relative to the propagation direction, electrode tissue distances as well as clinical filter settings. Catheter signals are computed on a realistic 3D catheter geometry using bidomain simulations of cardiac electrophysiology. Thereby high conductivities of the catheter electrodes are taken into account. For validation, simulated electrograms are compared with in vivo electrograms recorded during an EP-study with direct annotation of catheter orientation and tissue contact. Good agreement was reached regarding timing and signal width of simulated and measured electrograms. Correlation was** $0.92 \pm 0.07$ **for bipolar,** $0.92 \pm 0.05$ **for unipolar distal and** $0.80 \pm 0.12$ **for unipolar proximal electrograms for different catheter orientations and locations.**

## I. Introduction

Measurement and interpretation of intracardiac electrograms (IEGM) is an important diagnostic mean in today's electrophysiologic procedures. Information extracted from these signals, measured by a catheter electrode gently positioned at the cardiac wall, offer guidance in treatment of cardiac arrhythmias, whereof atrial fibrillation is the most common one.

Morphology of IEGM can reveal information about direction and velocity of the depolarisation front [1]. Moreover, it can possibly characterize the underlying substrate, which can be studied by biosignal analysis [2] and automatic classification [3]. These relevant diagnostic parameters are superimposed by changes in signal morphology due to catheter position and orientation as well as filter settings. In order to support clinical diagnosis a proper understanding of the influence of these system related parameters is essential.

Recent publications present the state of the art in human atrial modeling. Physiological as well as pathological conditions regarding cellular models and atrial excitation can be accurately modeled [4]. In silico modeling of atrial fibrillation is adressed e.g. by Aslanidi et al. [5] and Uldry et al. [6]. A comparison of atrial models published until today is given by Wilhelms et al. [7]. To conclude, it can be stated, that in-silico modeling of the human heart is moving towards an advanced level, which brings out the predictive potency of electrophysiologic simulations.

In order to study the genesis of IEGM and its link to atrial excitation patterns, several approaches have been presented. In most cases, extracellular potentials were calculated from transmembrane voltages or currents using a current source approximation [8], [9] or boundary element methods [10]. As an input for these calculations, monodomain simulations or simulations with cellular automata were used to describe cardiac excitation. We compared the results of monodomain with bidomain simulations and found small differences. Simulations using the bidomain model showed better correspondence to measured signals [11]. Bidomain simulations are capable of modeling interactions between transmembrane voltages and the extracellular field distribution, and hence conductivities in extracellular space. Therefore, they can account for interactions between extracellular loads and reproduce the bending of the wavefront at the tissue blood boundary. Even monophasic action potentials have been studied with this approach [12]. However, most simulation studies lack a direct comparison to clinically measured data. In this article, we compare simulated with annotated clinical EGM. A focus is put on (a) the catheter tilt angle relative to the propagation direction (b) the distance between electrode and tissue and (c) the influence of a standard clinical filter setting on signal morphology.

## II. Methods

### A. Simulation setups

In this study the influence of different catheter angles, locations and filter settings on the IEGM morphology were studied in a geometrically detailed setting. Basic components of the simulation setup were the same as in [11]. A blood filled volume contained a rectangular flat sheet of myocardium (42.2 mm x 15 mm x 4.4 mm, see figure 1).

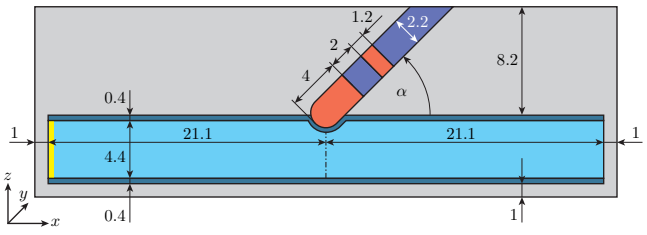


Fig. 1. Tip of a 7F catheter with two electrodes (red), separated by insulation (blue), rectangular piece of myocardium (light blue), setup filled with blood, extent of myocardial sheet in y-direction: 15 mm, myocardium is covered by an endothelial layer (dark blue), unit of all lengths depicted is mm, yellow bar indicates the stimulus position.

*The work of Matthias W Keller is supported by the German Research Foundation (DFG)

[1]Institute of Biomedical Engineering, Karlsruhe Institute of Technology (KIT), Karlsruhe, Germany publications@ibt.kit.edu
[2]Städtisches Klinikum Karlsruhe, Karlsruhe Germany

Wall thickness was chosen to represent a thick portion of the atrial wall [13]. Catheter electrodes were modeled as areas of high conductivity forming an equipotential surface. One set of simulations included several catheter tilt angles relative to the x-axis of the simulation setup (see Figure 4 for specific angles). In three setups we reproduced a clinical set of signals with different distances between catheter and tissue (Distances: 0 mm, -1.2 mm (indented), +5 mm (no contact), tilt angle $\alpha = 90°$). A thin layer of passive tissue was placed at the top and the bottom of the myocardial sheet to model a thin layer of endothelium. The geometry consisted of cubical voxels with a spatial resolution of 0.2 mm.

### *B. Simulation parameters and calculation of IEGM leads*

Bidomain simulations using the software aCELLerate [14] directly produced transmembrane voltages and extracellular potentials. For more detailed description of methods and equations see [11]. We previously showed, that in our small scale geometry the bidomain simulation, which produces a curved wavefront, results in a more accurate representation of the signal morphology of IEGM [11]. The human atrial cell model by Courtemanche et al. [15] was used. Myocardial extracellular conductivity was 0.199 S/m. The intracellular value was adjusted to 0.3 S/m in order to receive a conduction velocity (CV) of 1.0 m/s, which is in the range reported for human atria [1]. Tissue conductivity was assumed to be isotropic. For activation, a short stimulus with an intracellular current of 90 pA/pF for 2 ms was introduced at the left side of the myocardial sheet (see figure 1).
Extracellular potentials on the distal and proximal electrodes ($\phi_{e,p}(t)$ and $\phi_{e,d}(t)$) served as an input to calculate unipolar and bipolar signals. Unipolar signals were defined against a reference potential given by the mean of all extracellular potentials in the top layer of the setup. The definition of bipolar signals $v_{bip}(t)$ was the difference of proximal and distal signals: $v_{bip}(t) = \phi_{e,p}(t) - \phi_{e,d}(t)$.

### *C. Acquisition of clinical signals*

During ablation procedures, catheter signals were annotated and exported digitally from the recording system (LabSystem PRO EP, Bard, USA). From a four electrode ablation catheter (Blazer Prime XP, Boston Scientific, USA), electrode 1 (distal) and electrode 2 signals were acquired with a sampling frequency of 1 kHz. Signals were filtered with a standard clinical bandpass filter (30-250 Hz). All signals were recorded during pacing from the coronary sinus at a basic cycle length of 600 ms. Catheter position was determined by visual inspection of fluoroscopic images. For each position 20 s of signal were exported for analysis. As a stable catheter position had to be established, catheter angle was not chosen freely, but resulted from geometrical constraints of the recording position. In this study we use five annotated sets of electrograms from one patient for direct comparison with simulated EGM.

### *D. Processing of clinical data and signal comparison*

For comparison a representative mean signal was created from each 20 s recording. Therefore active segments were detected using a segmentation algorithm, which is based on the nonlinear energy operator and adaptive thresholding [16]. Only those segments that matched the pacing frequency were taken into account. Extracted segments were first aligned by maximum correlation and afterwards a mean signal was calculated (see figure 6). For comparison, simulated EGM, which matched the time delay of the unipolar leads and therefore the tilt angle of clinical signals, were chosen. They were filtered using a Butterworth filter and the same cutoff frequencies as in the clinical setting (30-250 Hz). Similarity of measured and simulated signals was quantified by calculating the correlation coefficient between the mean signal and corresponding simulated EGM.

## III. Results

### *A. Catheter angle variation*

In figure 2 the distribution of extracellular potentials on, and surrounding the catheter electrodes is visualized. While

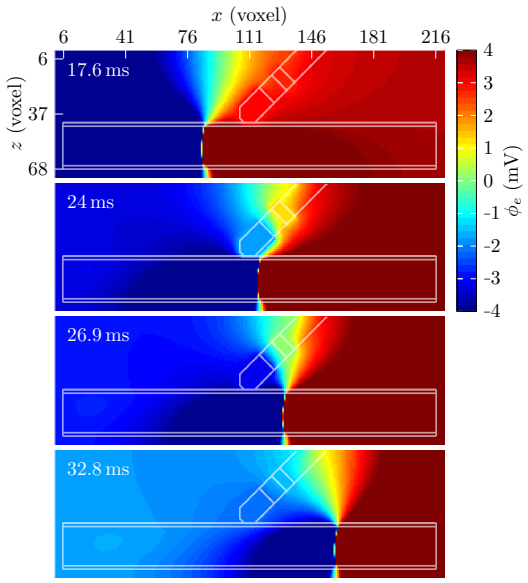


Fig. 2. Time sequence of extracellular potentials; A depolarisation front is passing underneath the catheter. The wavefront is curved due to bath loading effects. Especially at timepoint 24 ms the influence of the equipotential surfaces of the electrode on the potential distribution becomes visible. The field distortion of the distal electrode influences the proximal electrode.

the wavefront is passing, the distal electrode distorts the potential on the proximal electrode. This leads to a dip in the positive or negative deflection of proximal electrograms for steep angles ($<45°$ and $>135°$, see figure 3). Figures 3 and 4 show simulated signals for different catheter angles. Only minor changes occure in the distal lead, which is the turning point for all setups. For the proximal signal a continuous change is visible. Corresponding catheter positions, which are symmetric to the 90 ° position show a certain symmetry of the signal morphology. However, the 0° and 180° signals are not perfectly symmetric. For different catheter angles, bipolar signal morphology changes from monophasic signals with only one deflection to symmetric biphasic signals for the orhogonal position.

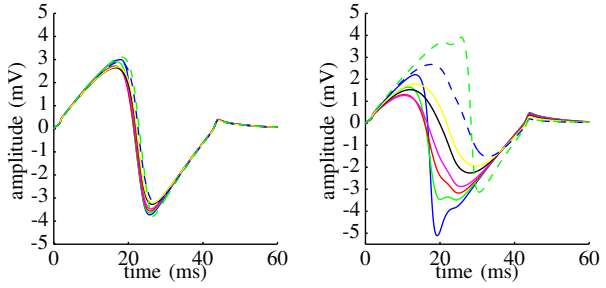


Fig. 3. Simulated unipolar electrograms for several catheter angles distal (left) proximal (right). Legend see figure 4.

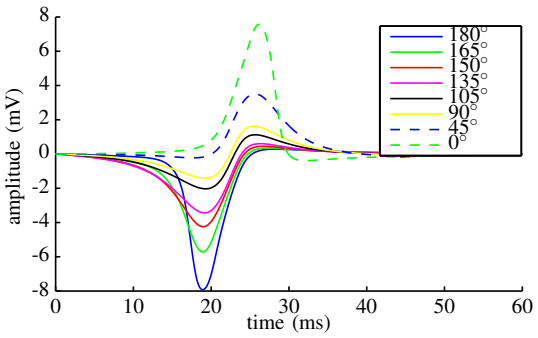


Fig. 4. Simulated bipolar electrograms for several catheter angles.

### B. Filtering signals

On first sight the presented clinical signals and the simulated signals look hardly similar. However, after applying the bandpass a significant change occurs (see figure 5). The bipolar signal morphology changes from a monophasic

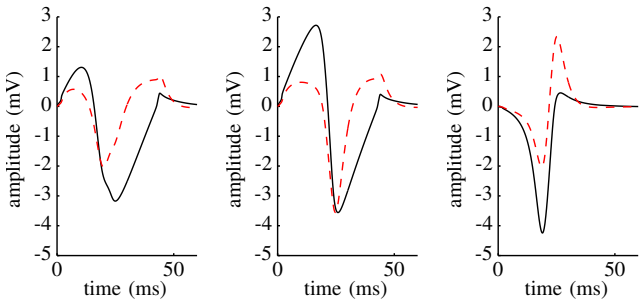


Fig. 5. The effect of a clinical standard filter (30 Hz-250 Hz); unipolar proximal (left), unipolar distal (middle) and bipolar (right) leads. Unfiltered (black, solid) and filtered (red, dashed) simulated EGM, catheter angle $\alpha = 150°$

negative deflection to a nearly symmetric biphasic one. Unipolar signals change from biphasic to triphasic, which shows the differentiating behavior of the clinical filter setting.

### C. Comparison to clinical data for different catheter angles

As one example bipolar leads of a simulation and a mean measured signal for a catheter angle of 150° are shown in figure 6. Quantative comparison of other orientations are shown in table I. The width of the electrogram as well as polarity and symmetry of the positive and negative deflection are similar. Amplitudes differ by 1 mV for each deflection. Morphological similarity of measurement and simulation is

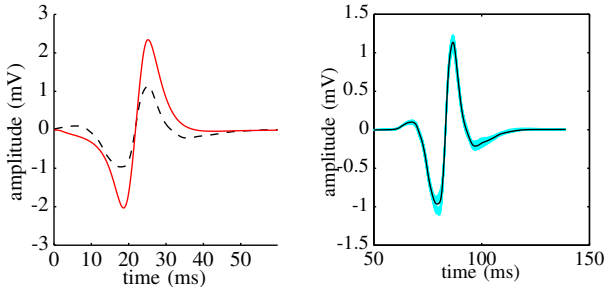


Fig. 6. left: Comparison of bipolar measured (red, solid) and simulated (black,dashed) EGM, catheter angle $\alpha = 150°$; right: Generation of a mean signal (black) from several measured electrograms (cyan).

TABLE I

CORRELATION COEFFICIENTS OF SIMULATED AND MEASURED SIGNALS

| | bipolar | distal | proximal |
|---|---|---|---|
| $\alpha = 150°$ touching | 0.96 | 0.96 | 0.94 |
| $\alpha = 165°$ touching | 0.81 | 0.97 | 0.90 |
| $\alpha = 90°$ touching | 0.96 | 0.91 | 0.70 |
| $\alpha = 90°$ indented | 0.97 | 0.94 | 0.76 |
| $\alpha = 90°$ no contact | 0.90 | 0.84 | 0.68 |

quantified by correlation coefficients, which are displayed in table I. For all leads the correlation coefficient exceeds 0.94. This implies a high similarity in terms of morphology and timing of the leads. For a better visual comparison of timing and morphology as well as amplitude ratios of different leads, signals were scaled. All leads were scaled with the same scaling factor. The scaling factor was determined in a way that the positive deflection of the bipolar electrograms obtains an amplitude of 1 (see figure 7).

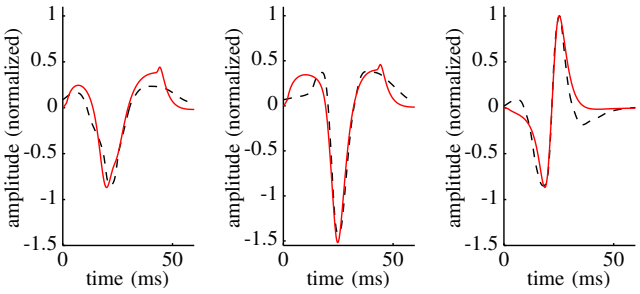


Fig. 7. Comparison of unipolar proximal (left), unipolar distal (middle) and bipolar (right) leads. Measured (black, dashed) and simulated (red, solid) EGM. Catheter angle $\alpha = 150°$.

### D. Distance between electrode and tissue (angle $\alpha = 90°$)

A comparison of changes in amplitude and peakedness of bipolar measured and simulated signals is presented in figure 8. Simulated signals were filtered as described previously and aligned in time at the point of the positive maximum for easier visual comparison. As seen before, amplitudes of the measured signals are smaller in the presented clinical dataset than those of the simulated signals. A pairwise correlation of corresponding signals is shown in table I. For distal and bipolar EGM correlation is high. However, for proximal EGM, the correlation is clearly smaller.

Comparing different catheter locations, signal width only shows little changes, whereas the peakedness is clearly increased for stronger tissue contact. This is linked to a higher frequency content of these signals.

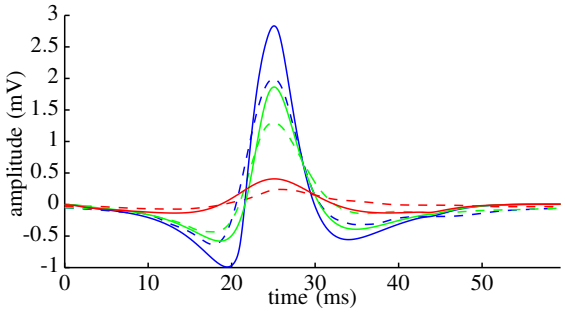


Fig. 8. Measured (dashed) and simulated (solid) signals for different electrode tissue distances. Blue: indented, green: touching, red: no contact.

## IV. Discussion and conclusions

In this contribution bidomain simulations of IEGM on a detailed 3D catheter geometry were presented. For a number of different catheter positions filtered simulated signals show high correlation with measured clinical signals. This statement holds for both distal and proximal signals, and thus also for bipolar signals.

The simulated amplitudes reach up to a peak-to-peak value of 8 mV compared to 4 mV for the measured dataset. Several parameters can account for this difference. One unknown parameter for the clinical data is the wall thickness, which can be thinner than one millimeter in some areas. Reducing the tissue thickness in simulations by half, leads to a decrease of a few millivolts in amplitude. Also, using different cell models or changing the intracellular conductivity can vary the amplitude. Finally, a point of discussion is the description of the electrode tissue interface, which was treated like an ideal non-polarizable electrode in our case.

Simulated signal width and timing between different leads was closely matched. This is resembled in high correlation coefficients between measured and simulated EGM. Only for proximal EGM at an angle of 90° correlation was decreased. This might be related to the proximity of these electrodes to the border of the simulation setup. The main part of the signal was nearly identical for several cases. However, start and end of the measured bipolar electrograms for $\alpha = 150°$ show small deflections, which are not reproduced by the simulation.

We recognize how important it is to consider the highpass and lowpass setting of the filter for an interpretation of the shape of the electrogram. In particular, small changes in the highpass cutoff frequency change the slope and morphology of the signal tremendously. Therefore, information about starting and end potentials as e.g. presented by Wiener et. al. [17] could get completely lost. Our simulations showed a visible dip in proximal signals for steep catheter angles, produced by a field distortion of the distal electrode. Unfiltered clinical signals should help to verify this effect in clinical data.

Our study showed that catheter orientation and location are highly relevant for the analysis of IEGM. Considering these parameters in algorithms for automatic analysis may improve the outcome of clinical procedures.

Future work will regard the impact of CV on electrogram width. Moreover, the influence of catheter orientations not perpendicular to the wavefront on the bipolar signal amplitude will be studied. Furthermore it is possible to include changes in substrate (e.g. fibrosis) to gain further insight about the genesis of complex fractionated EGM and other pathological conditions.

## References

[1] F. M. Weber, C. Schilling, G. Seemann, A. Luik, C. Schmitt, C. Lorenz, and O. Dössel, "Wave-direction and conduction-velocity analysis from intracardiac electrograms–a single-shot technique," IEEE TBME, 57(10), 2394–2401, 2010.

[2] C. Schilling, A. Luik, M. W. Keller, C. Schmitt, and O. Dössel, "Characterizing continuous activity with high fractionation during atrial fibrillation," in Proc. 7th International Workshop on Biosignal Interpretation, 1-2 July, Palace Hotel, Como, Italy, pp. 49–52, 2012.

[3] V. Kremen, L. Lhotska, M. Macas, R. Cihak, V. Vancura, J. Kautzner, and D. Wichterle, "A new approach to automated assessment of fractionation of endocardial electrograms during atrial fibrillation," Physiol Meas, 29(12), 1371–1381, 2008.

[4] O. Dössel, M. W. Krueger, F. M. Weber, M. Wilhelms, and G. Seemann, "Computational modeling of the human atrial anatomy and electrophysiology," MBEC, 50(8), pp. 773–799, 2012.

[5] O. V. Aslanidi, M. Al-Owais, A. P. Benson, M. Colman, C. J. Garratt, S. H. Gilbert, J. P. Greenwood, A. V. Holden, S. Kharche, E. Kinnell, E. Pervolaraki, S. Plein, J. Stott, and H. Zhang, "Virtual tissue engineering of the human atrium: Modelling pharmacological actions on atrial arrhythmogenesis," Eur J Pharm Sci, 2011.

[6] L. Uldry, V. Jacquemet, N. Virag, L. Kappenberger, and J. - M. Vesin, "Estimating the time scale and anatomical location of atrial fibrillation spontaneous termination in a biophysical model," Med Biol Eng Comput, 50(2), 155–163, 2012.

[7] M. Wilhelms, H. Hettmann, M. M. C. Maleckar, J. T. Koivumäki, O. Dössel, and G. Seemann, "Benchmarking electrophysiological models of human atrial myocytes," Front Physiol, 3(487), 2013.

[8] V. Jacquemet, N. Virag, Z. Ihara, L. Dang, O. Blanc, S. Zozor, J. - M. Vesin, L. Kappenberger, and C. Henriquez, "Study of unipolar electrogram morphology in a computer model of atrial fibrillation," J Cardiovasc Electrophysiol, 14(10 Suppl), pp. 172–9, 2003.

[9] U. Richter, L. Faes, A. Cristoforetti, M. Mase, F. Ravelli, M. Stridh, and L. Sornmo, "A novel approach to propagation pattern analysis in intracardiac atrial fibrillation signals," Ann Biomed Eng, 39(1), pp. 310–323, 2011.

[10] X. Zhu, and D. Wei, "Computer simulation of intracardiac potential with whole-heart model," Int J Bioinform Res Appl, 3(1), pp. 100–122, 2007.

[11] M. W. Keller, S. Schuler, G. Seemann, and O. Dössel, "Differences in intracardiac signals on a realistic catheter geometry using mono and bidomain models," in Computing in Cardiology, Krakow, Vol. 39, pp. 305–308, 2012

[12] J. V. Tranquillo, M. R. Franz, B. C. Knollmann, A. P. Henriquez, D. A. Taylor, and C. S. Henriquez, "Genesis of the monophasic action potential: role of interstitial resistance and boundary gradients," Am J Physiol Heart Circ Physiol, 286(4), 1370, 2004.

[13] K. Otomo, K. Uno, H. Fujiwara, M. Isobe, and Y. Iesaka, "Local unipolar and bipolar electrogram criteria for evaluating the transmurality of atrial ablation lesions at different catheter orientations relative to the endocardial surface," Heart Rhythm, 7(9), pp. 1291–1300, 2010.

[14] G. Seemann, F. B. Sachse, M. Karl, D. L. Weiss, V. Heuveline and O. Dössel, "Framework for modular, flexible and efficient solving the cardiac bidomain equation using PETSc," Mathematics in Industry, 15(2), 363–369, 2010.

[15] M. Courtemanche, R. J. Ramirez, and S. Nattel, "Ionic mechanisms underlying human atrial action potential properties: Insights from a mathematical model," Am. J. Physiol., 275(1 Pt 2), pp. H301–H321, 1998.

[16] M. P. Nguyen, C. Schilling, and O. Dössel, "A new approach for automated location of active segments in intracardiac electrograms," in IFMBE Proceedings World Congress on Medical Physics and Biomedical Engineering, Vol. 25/4, pp. 763–766, 2009.

[17] T. Wiener, F. O. Campos, G. Plank, and E. Hofer, "Decomposition of fractionated local electrograms using an analytic signal model based on sigmoid functions," Biomed Tech (Berl), 57(5), pp. 371-382, 2012.